X-ray Diffraction and 2D Gradient-Assisted $^{1}H-^{119}Sn$ HMQC NMR Studies of Structures Obtained from Nucleophilic Substitutions on Dimethyltin(IV) Salicylaldoximates

Rudolph Willem,*[,†,‡,§] Abdeslam Bouhdid,[§] Abdelkrim Meddour,[†,§] Carlos Camacho-Camacho,[§,||] Frédéric Mercier,[†,§] Marcel Gielen,[§] and Monique Biesemans[†,§]

High Resolution NMR Centre (HNMR) and Laboratory of General and Organic Chemistry of the Faculty of Applied Sciences (AOSC), Free University of Brussels (VUB), Pleinlaan 2, B-1050 Brussel, Belgium

François Ribot and Clément Sanchez

Laboratoire de Chimie de la Matière Condensée, URA CNRS 1466, Tour 54, 5e étage, Université Pierre et Marie Curie, 4 Place Jussieu, F-75252 Paris Cedex 05, France

Edward R. T. Tiekink

Department of Chemistry, The University of Adelaide, South Australia 5005, Australia

Received May 7, 1997[⊗]

The reactivity of the trinuclear tin cluster $[(Me_2Sn)_2(Me_2SnO)(OCH_3)(HONZO)(ONZO)]$ (**3a**; HONZOH = *o*-HON=CH-C_6H_4-OH, salicylaldoxime) toward proton-donating nucleophiles is investigated with the purpose of studying the influence of the nature and acidity of the entering nucleophile on the reactivity of **3a** and the stability of its cluster network. Reactions of **3a** with benzaldoxime, HON=CH-C_6H_5, and phenols HO-$C_6H_{5-n}X_n$ ($pK_a > 8$) preserve the cluster network and give rise to smooth substitution of the μ_2-OCH_3 moiety for, respectively, a μ_2-bridging benzaldoximate, generating $[(Me_2Sn)_2(Me_2SnO)(ONCHC_6H_5)$-(HONZO)(ONZO)] (**4**), and μ_2-bridging phenolates, generating $[(Me_2Sn)_2(Me_2SnO)$-$(OC_6H_{5-n}X_n)(HONZO)(ONZO)]$ (n = 1, X = 4-Me (**5a**), 4-Br (**5b**), 3-Cl (**5c**), 3-NO_2 (**5d**); n = 2, 3,5-Me_2 (**5e**)). More acidic or sterically hindered ortho-disubstituted phenols lead to decomposition of the trinuclear cluster or to mixtures from which no pure trinuclear cluster can be isolated. Reactions of **3a** with carboxylic acids, acetic and *p*-toluic acids, and acetylacetone lead to clean decomposition of the trinuclear cluster, yielding the respective bis[dicarboxylatotetramethyldistannoxanes], **6a** and **6b**, and dimethyltin bis(acetylacetonate), $Me_2Sn(acac)_2$, **7**. Reaction of **3a** with ethylene glycol generates a mixture of trinuclear clusters, from which 1,3-dioxa-2,2-dimethyl-2-stannacyclopentane (**8a**) precipitates. Crystal structure determinations by X-ray diffraction for **4**, **5a**, and **5b** reveal essentially the same trinuclear clusters as in **3a** and related compounds, with a seven-coordinate pentagonal-bipyramidal tin atom linked to two five-coordinate trigonal-bipyramidal tin atoms via a network of oxygen atoms. All new trinuclear tin clusters have been characterized in solution by gradient-assisted 2D NMR.

Introduction

Novel structures resulting from condensation reactions of a diorganotin(IV) oxide, R_2SnO (R = n-Bu,[1a] Me[1b]), with salicylaldoxime, *o*-HON=CHC_6H_4-OH, hereafter HONZOH, have recently been elucidated[1] by X-ray diffraction and gradient-assisted[2] 2D $^{1}H-^{13}C$ and $^{1}H-^{119}Sn$ HMQC[3a]/HMBC[3b,c] NMR spectroscopy.[4] These compounds are small clusters displaying two unequivalent salicylaldoximate and three diorganotin moieties

† High Resolution NMR Centre, Free University of Brussels.

‡ E-mail: rwillem@vub.ac.be.

§ Laboratory of General and Organic Chemistry of the Faculty of Applied Sciences, Free University of Brussels.

|| Present address: Universidad Autónoma Metropolitana−Xochimilco, Departamento de Sistemas Biológicos, Calzada del Hueso, 1100 Col. Villa Quietud, C.P. 04960, Mexico D.F.

⊗ Abstract published in *Advance ACS Abstracts,* August 15, 1997.

(1) (a) Kayser, F.; Biesemans, M.; Bouâlam, M.; Tiekink, E. R. T.; El Khloufi, A.; Meunier-Piret, J.; Bouhdid, A.; Jurkschat, K.; Gielen, M.; Willem, R. *Organometallics* **1994**, *13*, 1098, 4126. (b) Willem, R.; Bouhdid, A.; Kayser, F.; Delmotte, A.; Gielen, M.; Martins, J. C.; Biesemans, M.; Mahieu, B.; Tiekink, E. R. T. *Organometallics* **1996**, *15*, 1920.

(2) (a) Keeler, J.; Clowes, R. T.; Davis, A. L.; Laue, E. D. *Methods Enzymol.* **1994**, *239*, 145. (b) Tyburn, J.-M.; Bereton, I. M.; Doddrell, D. M. *J. Magn. Reson.* **1992**, *97*, 305. (c) Ruiz-Cabello, J.; Vuister, G. W.; Moonen, C. T. W.; Van Gelderen, P.; Cohen, J. S.; Van Zijl, P. C. M. *J. Magn. Reson.* **1992**, *100*, 282. (d) Vuister, G. W.; Boelens, R.; Kaptein, R.; Hurd, R. E.; John, B. K.; Van Zijl, P. C. M. *J. Am. Chem. Soc.* **1991**, *113*, 9688.

(3) (a) Bax, A.; Griffey, R. H.; Hawkins, B. L. *J. Magn. Reson.* **1983**, *55*, 301. (b) Bax, A.; Summers, M. F. *J. Am. Chem. Soc.* **1986**, *108*, 2093. (c) Bax, A.; Summers, M. F. *J. Magn. Reson.* **1986**, *67*, 565.

(4) (a) Kayser, F.; Biesemans, M.; Gielen, M.; Willem, R. *J. Magn. Reson.* **1993**, *A102*, 249. (b) Martins, J. C.; Verheyden, P.; Kayser, F.; Gielen, M.; Willem, R.; Biesemans, M. *J. Magn. Reson.* **1997**, *124*, 218. (c) Kayser, F.; Biesemans, M.; Gielen, M.; Willem, R. In *Advanced Applications of NMR to Organometallic Chemistry;* Gielen, M., Willem, R., Wrackmeyer, B., Eds.; Wiley: Chichester, U.K., 1996; Chapter 3, pp 45−86.

S0276-7333(97)00378-6 CCC: $14.00

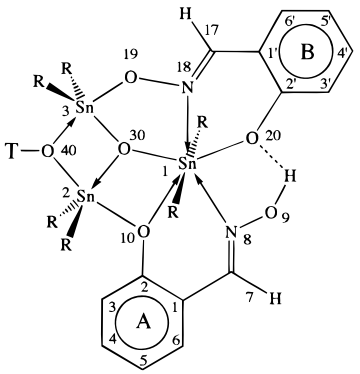

	T	R
1a	H	n-Bu
1b	HOZN	n-Bu
2a	H	Me
2b	HOZN	Me
3a	Me	Me
3b	Et	Me
3c	n-Pr	Me
3d	i-Pr	Me
4	HZN	Me
5a	p-Me-C_6H_4	Me
5b	p-Br-C_6H_4	Me
5c	m-Cl-C_6H_4	Me
5d	m-NO_2-C_6H_4	Me
5e	3,5-Me_2-C_6H_4	Me

Figure 1. General structure, with atom labeling, of compounds from several condensation reactions between di-*n*-butyl or dimethyltin(IV) oxide and salicylaldoxime, synthesized previously (**1a**, **1b**[1a] and **2b**, **3a**−**e**[1b]) or in the present work (**4**, **5a**−**e**). HOZN represents the salicylaldoximate moiety C bound to O40 by its nitrogen atom; HZN, accordingly represents the benzaldoximate moiety bound to O40 in the same way.

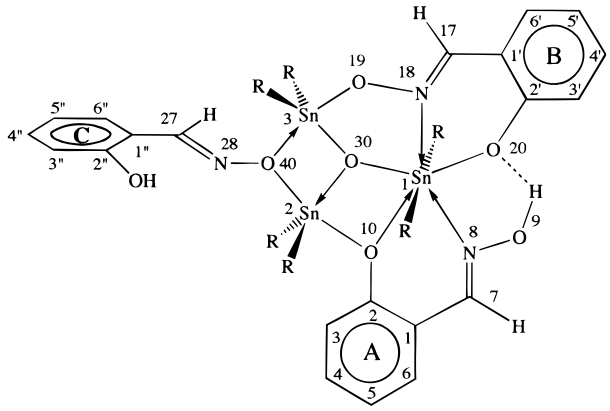

Figure 2. Solution structures of **1b** and **2b**.[1b]

linked by Sn−O−Sn bridges, with one seven-coordinate (Sn1) and two five-coordinate (Sn2 and Sn3) tin atoms (Figure 1).[1] The noncrystalline compounds $[(R_2Sn)_2(R_2SnO)(ONZOH)(HONZO)(ONZO)]$ (**1b**, R = *n*-Bu; **2b**, R = Me) (Figure 2) are the key intermediates in the synthesis of such clusters.[1b] Cyclohexane, hexane, acetonitrile, or methanol solutions of **1b** give rise to crystals having structure **1a** instead of **1b**.[1a] Compound **2b** gives rise to crystalline materials only from low molecular weight alcohols, T-OH (T = Me, Et, *n*-Pr, *i*-Pr), providing, respectively, compounds **3a**−**d** instead of **2b** or **2a**.[1b] These structural changes occur during the crystallizations according to the reaction in Scheme

Scheme 1

$$[(R_2Sn)_2(R_2SnO)(ONZOH)(HONZO)(ONZO)] + T\text{-}OH \longrightarrow [(R_2Sn)_2(R_2SnO)(OT)(HONZO)(ONZO)] + HONZOH$$

T = H, R = n-Bu; T = Me, Et, n-Pr, i-Pr, R = Me

1. The reversible reactions linking all these compounds are nucleophilic substitutions at the cluster site Sn2−O40−Sn3, where a μ_2-bridged T-O group is substituted for another μ_2-bridged W-O one, under proton transfer from the entering W-OH nucleophile toward the leaving T-OH one.[1] It thus appears that the proton donor properties of the entering nucleophile as well as the Sn2−O40−Sn3 bridging functionality entirely determine the reactivity of such clusters.

Whether all nucleophiles possessing transferable protons are amenable to such reactions and to which extent the acidity of the entering nucleophile is a critical factor remains to be established. The main purpose of the present paper is to report on the influence of the nature and acidity of the entering nucleophile on the reactivity of such compounds, more specifically, on the stability of their cluster network. It is aimed at defining the acidity limits within which smooth μ_2-bridged nucleophilic substitution with preservation of the cluster pattern is possible. To do so, we investigated the reactivity of the most stable of these clusters in solution, **3a**,[1b] toward a wide panel of proton-donating nucleophiles, phenols with various pK_a's, two carboxylic acids, acetylacetone, ethylene glycol, and benzaldoxime. A further motivation to investigating phenols and benzaldoxime is dictated by the noncrystalline **2b** in which tin atoms are bound to both the phenolic and oximic oxygens of the salicylaldoximate ligands. Since **2b** could not be obtained as a crystalline compound, it was interesting to investigate whether similar structures involving only one of these functions can be obtained in a form amenable to X-ray diffraction analysis.

Results and Discussion

Synthetic Aspects. Compound **3a**, $[(Me_2Sn)_2(Me_2SnO)(OCH_3)(HONZO)(ONZO)]$, is convenient for investigating nucleophilic substitutions because it is relatively stable and the leaving nucleophile, methanol, can easily be eliminated. This feature is important since attempts at purification of such clusters by chromatographic methods lead to decomposition.[1]

Reaction of **3a** with benzaldoxime generates a crystalline compound amenable to a more precise characterization of the oxime binding mode to the Sn2−O40−Sn3 moiety proposed from solution NMR studies for **1b** and **2b**. Compound **4**, represented as $[(Me_2Sn)_2(Me_2SnO)(ON{=}CH\text{-}C_6H_5)(HONZO)(ONZO)]$, was isolated as a crystalline compound after substitution in benzene of the μ_2-OCH_3 group from **3a** for a μ_2-ON=CH-C_6H_5 one, under addition of benzaldoxime (C_6H_5-CH=NOH) and elimination of methanol. It was characterized by X-ray diffraction analysis in the crystalline state and shown to have the same structure in solution by NMR (see below). A similar attempt to react **3a** with acetaldoxime, $CH_3CH{=}NOH$, failed since **3a** was recovered essentially quantitatively. This result emphasizes the importance of the proton transfer from the entering toward the leaving nucleophile, as the too low acidity of acetaldoxime hampers this.

Reacting phenols with **3a** is of interest for two reasons. First, since **3a** reacts with salicylaldoxime to form **2b**, with coordination through the oximic rather than the phenolic oxygen, it should be established whether a phenolic oxygen is likewise amenable to Sn2−O40−Sn3 bridging;[1] second, the role of the acidity degree of the entering phenols should be outlined.

Phenols react with **3a** in benzene at room temperature. The anticipated complexes have the general formula $[(Me_2Sn)_2(Me_2SnO)(OAr)(HONZO)(ONZO)]$. In the case of *p*-cresol ($pK_a = 9.82$), *p*-bromophenol ($pK_a = 9.34$), *m*-chlorophenol ($pK_a = 9.08$), *m*-nitrophenol ($pK_a = 8.38$), and 3,5-dimethylphenol ($pK_a = 10.15$), novel compounds **5a**−**e**, respectively (Figure 1), could be isolated as solids. For the *p*-cresol and *p*-bromophenol derivatives, **5a** and **5b**, crystals suitable for X-ray analysis were obtained. Their solid state and solution structures display essentially the same motifs as do the solution structures of **5c**−**e** (see NMR data below).

Two further features of the reaction of **3a** with phenols were assessed: steric effects and phenol acidity.

Reaction of **3a** with phenols appears sensitive to steric hindrance, since attempts under similar conditions to isolate $[(Me_2Sn)_2(Me_2SnO)(OAr)(HONZO)(ONZO)]$ from 2,6-dimethylphenol ($pK_a = 10.59$) and 2,4,6-trimethylphenol ($pK_a = 10.88$) did not provide the desired compounds in pure form. ^{119}Sn NMR analysis of the crude reaction mixture reveals that it contains only small quantities (*ca.* 10−20%) of the expected aryloxy complex, together with comparable amounts of **2b** and unreacted **3a**, as well as the other usual transients, m_2 and m_3.[1] As steric hindrance of the ortho substituents of the entering phenols hampers the formation of the desired aryloxy complex, it is likely that their acidity facilitates the conversion of **3a** to **2b**, through protonation of the μ_2-alkoxy group.[1a]

With phenols having a pK_a slightly lower than 8, no pure $[(Me_2Sn)_2(Me_2SnO)(OAr)(HONZO)(ONZO)]$ can be isolated from their reaction with **3a**. Thus, for *p*-cyanophenol ($pK_a = 7.95$) and *p*-nitrophenol ($pK_a = 7.16$), ^{119}Sn resonance analysis of the reaction mixtures obtained reveals the desired product together with **2b** and **3a**, in the approximate ratios 69:27:4 and 54:42:4, respectively, in addition to the usual minor species giving rise to noisy resonances.[1b] Thus, the threshold phenol pK_a, below which smooth substitution of the methoxy group of **3a** for a substituted phenoxy group is no longer possible, lies in the range 8.0−8.4. Again, acidity causes the undesired formation of **2b** from **3a** through facilitated proton transfer. That phenol acidity is determinant is further supported by the reaction of **3a** with 2,4-dinitrophenol ($pK_a = 4.09$), which leads to destruction of the cluster structure, as revealed by the collapse of the three ^{119}Sn resonance pattern characterizing such clusters.[1]

The role of the acidity in μ_2-nucleophilic substitutions on the Sn2−O40−Sn3 moiety of **3a** was further assessed by reactions of **3a** with carboxylic acids. Thus, the bidentate nature of carboxylates could *a priori* favor the formation of a carboxylate bridging the Sn2 and Sn3 atoms. On the other hand, the higher acidity of carboxylic acids, as compared to phenols, is an unfavorable premice. No cluster with bridging carboxylates of the type $[(Me_2Sn)_2(Me_2SnO)(OOCR')(HONZO)(ONZO)]$ was indeed obtained. Thus, reaction of **3a** with acetic acid

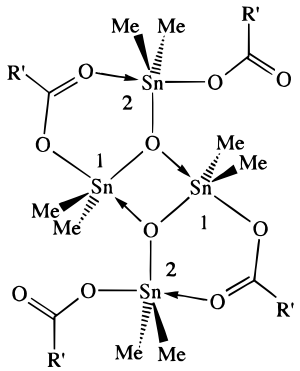

Figure 3. Solution state structure of dimeric bis[dicarboxylatotetramethyldistannoxanes] obtained from the reaction of **3a** with a carboxylic acid R′-COOH (R′ = CH_3, **6a**; *p*-CH_3-C_6H_4, **6b**).

Scheme 2

$$2\,[(Me_2Sn)_2(Me_2SnO)(OCH_3)(HONZO)(ONZO)] + 6\,R'\text{-}COOH + H_2O \longrightarrow (3/2)\,[(R'\text{-}COO)Me_2Sn\text{-}O\text{-}SnMe_2(OOC\text{-}R')]_2 + 2\,CH_3OH + 4\,HONZOH$$

6a: R′ = Me-
6b: R′ = p-Me-C_6H_4-

Scheme 3

$$[(Me_2Sn)_2(Me_2SnO)(OCH_3)(HONZO)(ONZO)] + 6\,acacH \longrightarrow 3\,Me_2Sn(acac)_2 + CH_3OH + 2\,HONZOH + H_2O$$

7

and *p*-toluic acid yielded dimeric bis[dicarboxylatotetraorganodistannoxanes], well-known compounds with a solution structure as shown in Figure 3.[5] In view of the results obtained with phenols, carboxylic acids thus have sufficient acidity to favor the decomposition of **3a** and the release of the dimethyltin oxide units needed for the generation of such dimeric bis[dicarboxylatotetraorganodistannoxanes], usually synthesized from condensation of a diorganotin oxide with a carboxylic acid in molar ratio 1:1.[5] In this picture, the formation of bis[diacetatotetramethyldistannoxane], **6a**, and bis[bis(4-methylbenzoato)tetramethyldistannoxane], **6b**, is readily explained by the stoichiometry shown in Scheme 2.

The X-ray structure of **6a** has been described previously by Lockhart and co-workers.[5a] Compound **6a**, synthesized, for comparison, by the usual reaction involving condensation of the carboxylic acid with dimethyltin(IV) oxide,[5] has physical characteristics identical to those obtained by scheme 3. Compounds **6a** and **6b** were characterized by elemental analysis and solution NMR.[10c]

Reaction of **3a** with 2,4-pentanedione (acetylacetone, acacH) yields bis(2,4-pentanedionato)dimethyltin(IV) ($(CH_3)_2Sn(acac)_2$, **7**). This result shows that the weak-

(5) (a) Lockhart, T. P.; Manders, W. F.; Holt, E. M. *J. Am. Chem. Soc.* **1986**, *108*, 6611. (b) Tiekink E. R. T. *Appl. Organomet. Chem.* **1991**, *5*, 1. (c) Tiekink, E. R. T. *Trends Organomet. Chem.* **1994**, *1*, 71. (d) Gielen, M.; Tiekink, E. R. T.; Bouhdid, A.; de Vos, D.; Biesemans, M.; Verbruggen, I.; Willem, R. *Appl. Organomet. Chem.* **1995**, *9*, 639. (e) Tiekink, E. R. T.; Gielen, M.; Bouhdid, A.; Biesemans, M.; Willem, R. *J. Organomet. Chem.* **1995**, *494*, 247. (f) Gielen, M.; Bouhdid, A.; Willem, R.; Bregadze, V. I.; Ermanson, L. V.; Tiekink, E. R. T. *J. Organomet. Chem.* **1995**, *501*, 277. (g) Gielen, M.; Biesemans, M.; El Khloufi, A.; Meunier-Piret, J.; Kayser, F.; Willem, R. *J. Fluorine Chem.* **1993**, *64*, 279. (h) Gielen, M.; El Khloufi, A.; Biesemans, M.; Kayser, F.; Willem, R. *Appl. Organomet. Chem.* **1993**, *7*, 201. (i) Gielen, M.; El Khloufi, A.; Biesemans, M.; Willem, R. *Appl. Organomet. Chem.* **1993**, *7*, 119. (j) Yano, T.; Nakashima, K.; Otera, J.; Okawara, R. *Organometallics* **1985**, *4*, 1501. (k) Dakternieks, D.; Jurkschat, K.; van Dreumel, S.; Tiekink, E. R. T. *Inorg. Chem.* **1997**, *36*, 2023.

Scheme 4

$[(Me_2Sn)_2(Me_2SnO)(OCH_3)(HONZO)(ONZO)] + 3\ HO\text{-}CH_2\text{-}CH_2\text{-}OH$

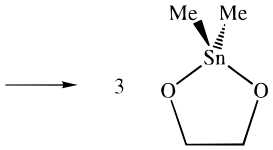

$+ 2\ HONZOH + CH_3OH + H_2O$

8a

ness of the acid (pK_a *ca.* 9, comparable to phenols)[6] is not a sufficient condition for μ_2-nucleophilic substitution on the Sn2−O40−Sn3 bridge of **3a** to be possible. Instead, the formation of the very stable bis-chelated, six-coordinate $(CH_3)_2Sn(acac)_2$ is thermodynamically favored according to Scheme 3. Compound **7** was easily characterized from comparison of its NMR spectral and physical characteristics with literature data.[7]

Lastly, **3a** was allowed to react with ethylene glycol in order to examine whether a diol is able to chelate the Sn2−O40−Sn3 unit of **3a**. A complex reaction mixture, from which a solid precipitates, was obtained. The solid is identified as 2,2-dimethyl-1,3-dioxa-2-stannacyclopentane (**8a**), generated as shown in Scheme 4. Only few data for the very poorly soluble **8a** were provided earlier.[8b] It was characterized here by solution ^1H and ^{119}Sn and solid state ^{13}C and ^{119}Sn NMR, mass spectrometry, and elemental analysis. Though less soluble, **8a** has properties comparable to those of the dibutyltin analog.[8a,c]

The evaporated filtrate of this reaction mixture could not be worked up to a pure product. It reveals the presence of approximately 22 ± 4% of **2a**, 48 ± 12% of **2b**, and 30 ± 8% of a new product, **8b**. *In situ* 2D gradient-assisted $^1H-^{119}Sn$ HMQC data[4] suggest a solution structure, $[(Me_2Sn)_2(Me_2SnO)(OCH_2\text{-})(HONZO)\text{-}(ONZO)]_2$, with an ethane diolate unit of which the two oxygens "μ_2-bridge" each a cluster unit at O40. No evidence was found for **8b** having a structure where a single ethylene glycol unit bridges the Sn2 and Sn3 atoms of a single cluster with each oxygen bound to a single tin atom.

X-ray Diffraction Structures of 4, 5a, and 5b. The molecular structures of **4** and **5a** shown in Figures 4 and 5, respectively, and that of **5b** (Figure S1, Supporting Information) closely resemble those found for **1a**[1a] and **3a**−**d**,[1b] and hence, a detailed description is not warranted. Accordingly, the bond lengths and angles given in Table 1 mainly refer to the bonding mode of the new ligand around the Sn2−O40−Sn3 bridge, the other data relevant to the remaining part of the cluster being available in the Supporting Information. The structures are isomorphous, and each unit cell comprises two tin-containing molecules and one solvent benzene molecule which is situated about a crystallographic center of inversion; there are no significant interactions between the constituents. The solvent molecules occupy channels parallel to the *c*-direction. The trinuclear cluster of **4** features the usual seven-coordinate Sn1 atom and two five-coordinate tin atoms, i.e., Sn2 and Sn3. The geometry about Sn1 is distorted pentagonal bipyramidal with the methyl substituents in axial positions. The pentagonal plane (planar to ±0.041 Å) is defined by the phenoxide oxygens and the oxime nitrogen atoms of the HONZO

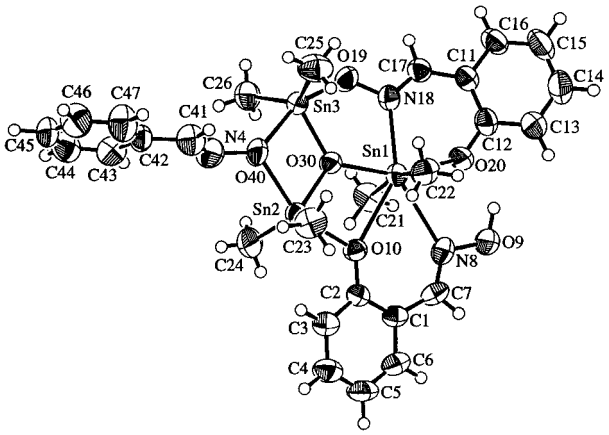

Figure 4. Molecular structure and crystallographic numbering scheme for $[(Me_2Sn)_2(Me_2SnO)(ONZH)(HONZO)\text{-}(ONZO)]$ (**4**) (HONZOH = salicylaldoxime, *o*-HON=CH-C_6H_4-OH; HONZH = benzaldoxime, HON=CH-C_6H_5).

Table 1. Selected Geometric Parameters for 4, 5a, and 5b

	compound		
	4	**5a**	**5b**
Bond Distances (Å)			
Sn(1)−O(10)	2.715(4)	2.695(4)	2.688(4)
Sn(1)−O(30)	2.177(4)	2.178(3)	2.181(4)
Sn(2)−O(10)	2.153(4)	2.145(4)	2.140(4)
Sn(2)−O(30)	2.002(4)	2.016(4)	2.006(4)
Sn(2)−O(40)	2.227(4)	2.204(4)	2.210(4)
Sn(2)−C(23)	2.120(7)	2.122(7)	2.097(7)
Sn(2)−C(24)	2.105(7)	2.122(7)	2.100(7)
Sn(3)−O(19)	2.083(5)	2.093(5)	2.090(5)
Sn(3)−O(30)	2.020(4)	2.010(4)	2.008(4)
Sn(3)−O(40)	2.248(5)	2.255(4)	2.274(4)
Sn(3)−C(25)	2.124(8)	2.106(7)	2.107(7)
Sn(3)−C(26)	2.116(7)	2.100(7)	2.096(7)
O(40)−N(4)[a]	1.403(7)	1.365(6)	1.372(6)
N(4)−C(41)	1.213(8)		
Bond Angles (deg)			
C(21)−Sn(1)−C(22)	164.6(3)	167.2(3)	166.3(3)
O(10)−Sn(2)−O(30)	80.1(1)	80.5(1)	80.6(2)
O(10)−Sn(2)−O(40)	153.8(2)	155.0(1)	154.9(2)
O(30)−Sn(2)−O(40)	74.1(2)	74.6(1)	74.4(1)
C(23)−Sn(2)−C(24)	134.3(3)	136.4(3)	135.4(3)
O(19)−Sn(3)−O(30)	86.9(2)	86.7(2)	87.8(2)
O(19)−Sn(3)−O(40)	159.9(2)	160.0(2)	160.5(2)
O(30)−Sn(3)−O(40)	73.3(2)	73.5(1)	72.9(2)
C(25)−Sn(3)−C(26)	135.2(3)	136.7(3)	137.8(3)
Sn(1)−O(10)−Sn(2)	95.1(1)	95.3(1)	95.4(2)
Sn(3)−O(19)−N(18)	121.2(3)	124.7(3)	123.6(4)
Sn(1)−O(30)−Sn(2)	119.5(2)	118.1(2)	118.0(2)
Sn(1)−O(30)−Sn(3)	126.5(2)	127.9(2)	127.1(2)
Sn(2)−O(30)−Sn(3)	114.0(2)	113.6(2)	114.7(2)
Sn(2)−O(40)−Sn(3)	97.8(2)	98.1(1)	97.8(1)
Sn(2)−O(40)−N(4)[a]	120.7(4)	129.7(3)	129.9(4)
Sn(3)−O(40)−N(4)[a]	122.3(4)	131.9(3)	131.8(4)
O(40)−N(4)−C(41)	116.2(7)		

[a] For structures **5a** and **5b**, N(4) is C(41).

(6) Carey, F. A. *Organic Chemistry*, 3rd ed.; McGraw-Hill: New York, 1996; p 736.

(7) (a) Miller, G. A.; Schlemper, E. O. *Inorg. Chem.* **1973**, *12*, 677. (b) McGrady, M. M.; Tobias, R. S. *J. Am. Chem. Soc.* **1965**, *87*, 1909. (c) Howard, W. F., Jr.; Crecely, R. W.; Nelson, W. H. *Inorg. Chem.***1985**, *24*, 2204. (d) Lockhart, T. P.; Manders, W. F. *Inorg. Chem.* **1986**, *25*, 892. (e) Manders, W. F.; Lockhart, T. P. *J. Organomet. Chem.* **1985**, *297*, 143. (f) Lockhart, T. P.; Manders, W. F.; Zuckerman, J. J. *J. Am. Chem. Soc.* **1985**, *107*, 4546. (g) Herber, R. H.; Leahy, M. F.; Hazony, Y. *J. Chem. Phys.* **1974**, *60*, 5070.

(8) (a) Davies, A. G.; Price, A. J.; Dawes, H. M.; Hursthouse, M. B. *J. Chem. Soc., Dalton Trans.* **1986**, 297. (b) Satai, S.; Fujimura, Y.; Ishii, Y. *J. Org. Chem.* **1970**, *35*, 2344. (c) Grindley, T. B.; Wasylishen, R. E.; Thangarasa, R.; Power, W. P.; Curtis, R. D. *Can. J. Chem.* **1992**, *70*, 205.

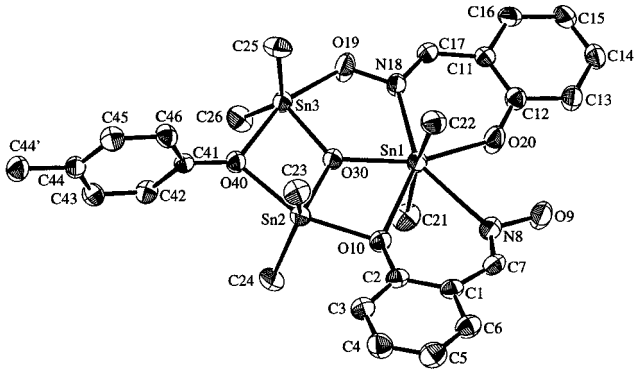

Figure 5. Molecular structure and crystallographic numbering scheme for $[(Me_2Sn)_2(Me_2SnO)(O\text{-}C_6H_4\text{-}CH_3)(HONZO)(ONZO)]$ (**5a**). An analogous numbering scheme is used for **5b**.

and ONZO anions as well as the O30) atom, which links Sn1 to the Sn2 and Sn3 atoms; the Sn1 lies 0.0145(4) Å above the basal plane in the direction of the C22 atom. The Sn2 and Sn3 atoms each exist in distorted trigonal-bipyramidal geometries with the Sn2 (Sn3) atom lying 0.0794(4) Å (0.1181(5) Å) out of the C_2O30 plane in the direction of the O10 (O19) atom. A difference map calculated toward the end of the refinement revealed the presence of a hydrogen atom on O9, consistent with the earlier studies,[1] and hence the assignment of the uninegative HONZO and dinegative ONZO anions is unambiguous. The O−H moiety is involved in an intramolecular hydrogen bonding contact to the O(20) atom of 1.77 Å. The C_6H_5-CH=NO residue is symmetrically disposed with respect to the cluster as seen in the Sn2/O40/N4/C41 and Sn3/O40/N4/C41 torsion angles of 125.9(6) and −109.9(7)°, respectively, and in the dihedral angle between the Sn_2O_2 plane and the plane through the C_6H_5-CH=NO atoms of 95.4°.

The structure of compound **4**, more specifically the binding mode of the bridging oximic oxygen atom, compares well with that proposed from solution NMR data for **1b** and **2b** (Figure 2).[1b] In particular, the structural arrangement where the salicylaldoximate ligand C in **1b** and **2b** and the benzaldoximate ligand in **4** are perpendicular to the mean plane through the cluster, comprising the network of Sn−O−Sn bridges and the ligands A and B, is noticeably common to the three compounds. The *E* configuration of the PhCH=NO moiety of **4** is, however, in contrast with the *Z* configuration in **1b** and **2b** proposed earlier on the basis of infrared data.[1b] Because of this configuration difference, the structure of **4** cannot be considered as an indirect support for the existence of a hydrogen bridge in **1b** and **2b**. Consequently, it is no longer represented in Figure 2.

The basic framework and coordination geometries of **4** are retained in both **5a** and **5b**, the main difference being the nature of the function bridging the Sn2 and Sn3 atoms (Figure 5). The substituted phenoxide functions are effectively orthogonal to the Sn_2O_2 plane as seen in the Sn2/O40/C41/C42 and Sn3/O40/C41/C42 torsion angles of, respectively, −89.2(6) and 98.3(6)° for **5a** and −90.9(7) and 99.0(6)° for **5b**. The similarity between **5a** and **5b** is not surprising given their very close pK_a's.

The geometric parameters in the structure of **4** are closer to those of **5a,b** than those of **3a**−**d**, reflecting different conjugation abilities of the T substituents. The Sn−O40 bond lengths are larger in **4** than the corresponding ones in **3a**−**d**, and the expansion in the Me−Sn2−Me and Me−Sn3−Me angles is also apparent. A further difference between **4** and the other structures relates to the geometry about the O40 atom, which is essentially trigonal planar in **1a**, **3a**−**d**, and **5a,b**. In **4**, the O40 atom lies 0.461(5) Å out of the plane defined by the Sn2, Sn3, and N4 atoms, and the sum of the angles subtended at O40 is 340.8°. This indicates that, for the benzaldoximate, a significant resonance contributor has the formal negative charge located on the oxygen atom, while for the phenoxides a significant contributing resonance structure would have a formal C=O. Experimental evidence for this is found by the presence of a very short N=C bond distance [1.213(8) Å] in **4**. Noticeable is also the more symmetrical bridge in **5a** than in **5b**.

NMR Studies on the Solution State Structures of 4, 5a−**e, and 8b.** An overview of the main NMR data of **4**, **5a**−**e**, **8b** in $CDCl_3$ solution is given in Table 2; the other data are given in the Experimental Section. The NMR signal assignment, obtained by a combination of gradient-assisted[2] 2D $^1H-^{119}Sn$ HMQC[3a,4] and $^1H-^{13}C$ HMBC spectroscopy,[3b,c] will not be detailed, since very similar $^1H-^{119}Sn$ HMQC and $^1H-^{13}C$ HMBC patterns were processed here with the same strategy for **4**, **5a**, and **8b** as for **1a**,[1a] **1b**,[1a,1b] **2b**,[1b] and **3a**,**b**.[1b] The $^nJ(^1H-^{119}Sn)$ coupling constants determined from 2D $^1H-^{119}Sn$ HMQC correlations are identical in **4**, **5a**, and **8b** to within 1−2 Hz to the corresponding values in **1a**,[1a] **3a**,**b**, and **2b**.[1b] On the basis of the full assignment of the $SnMe_2$ groups achieved by $^1H-^{119}Sn$ HMQC spectroscopy for **5a**, the corresponding resonances of **5b**−**e** can be assigned by simple extrapolation. Likewise, on the basis of 2D $^1H-^{13}C$ HMBC spectra obtained for **5a**, **5c**, and **5d**, a similar resonance transposition was achieved to **5b** and **5e**, except for most of their aromatic ^1H resonances subject to complex overlapping.

The structures of **4** and **5a** are identical in the solution and solid states. The key data to support this conclusion as well as to identify the solution structure of **8b** in its crude reaction mixture are the observation of 2D $^nJ(^1H-^{119}Sn)$ HMQC correlations between the $^{119}Sn2$ and $^{119}Sn3$ nuclei and some ^1H nuclei of the O40-bound organic moiety. Thus, the 2D $^1H-^{119}Sn$ HMQC spectra exhibit a correlation peak between the $^{119}Sn2$ and $^{119}Sn3$ resonances and the ^1H resonance of the ortho protons of the *p*-methylphenyl moiety of **5a** ($^4J(^1H\text{-}o\text{-}C46/42-C41-O40-^{119}Sn2/Sn3) < 2$ Hz), of the oximic proton of the benzaldoxime moiety of **4** ($^4J(^1H41-C41-N4-O40-^{119}Sn2/Sn3) < 2$ Hz), and of the methylene protons of the ethylene glycol moiety of **8b** ($^{3/4}J(^1H_2C-^1H_2C-O40-^{119}Sn2/Sn3)$, a composite correlation). As an example, Figure 6 shows the cross sections, along the F2, ^1H chemical shift axis, of the 2D gradient-assisted $^1H-^{119}Sn$ HMQC spectrum obtained for **8b** in a mixture with **2a** and **2b**, at the ^{119}Sn resonance frequencies of the two five-coordinate tin atoms Sn2 and Sn3. They exhibit the correlations between the methylene proton resonances and the ^{119}Sn ones of the tin atoms Sn2 and Sn3, in addition to those from the cluster moiety.

The ^{119}Sn resonances of **2b** generated in solution as a minor species, as well as the resonances from the other

Table 2. ^{119}Sn, ^{13}C and ^{1}H NMR Data of the Dimethyltin Moieties of 4 and 5a−e from $CDCl_3$ Solutions and 8b from C_6D_6 Solution[a]

compd	moiety	$\delta(^{119}Sn)$[b]	$^{n}J(^{119}Sn-^{119/117}Sn)$[c]	$\delta(^{13}C)$[d]	$^{1}J(^{13}C-^{119/117}Sn)$[e]	$\delta(^{1}H)$[f]	$^{2}J(^{1}H-^{119}Sn)$
4	Me_2Sn1	−452.7	325[h]; 46[h]	15.0	1102/1056	1.15	113[g]
	Me_2Sn2	−128.0	100[h]; 51[h]	3.6	684/644	0.71	76[g]
	Me_2Sn3	−114.4	314;[h] 100[h]	1.1	649/609	0.70	77[g]
5a (pK_a 9.82)	Me_2Sn1	−452.1	328[h]; 60[h]	14.5	1099/1047	0.92	109[g]
	Me_2Sn2	−138.1	90[h]; 56[h]	3.7	660/630	0.93	73[g]
	Me_2Sn3	−123.6	324[h]; 91[h]	0.9	648/625	0.74	74[g]
5b (pK_a 9.34)	Me_2Sn1	−451.9	311[h]; nr[j]	14.8	1094/1043	0.90	103[i]
	Me_2Sn2	−133.1	90[h]; 49[h]	3.9	664/630	0.89	82/78
	Me_2Sn3	−119.5	300;[h] 92[h]	1.2	650/625	0.71	75/72
5c (pK_a 9.08)	Me_2Sn1	−451.0	299[h]; 46[h]	14.7	1090/1040	0.91	109[i]
	Me_2Sn2	−132.2	85[h]; 49[h]	4.1	645/616	0.93	73[i]
	Me_2Sn3	−118.6	297[h]; 85[h]	1.4	650/622	0.75	73[i]
5d (pK_a 8.38)	Me_2Sn1	−450.0	290[h]; nr[j]	14.7	1085/1042	0.93	108[i]
	Me_2Sn2	−127.6	89[h]; 43[h]	4.2	659/628	0.96	73[i]
	Me_2Sn3	−113.9	290[h]; 85[h]	1.5	647/621	0.57	74[i]
5e (pK_a 10.15)	Me_2Sn1	−452.2	321/311; 52[h]	15.0	1106/1055	1.10	112[i]
	Me_2Sn2	−138.1	86[h]; 52[h]	3.5	664/636	0.59	74[i]
	Me_2Sn3	−125.0	324/308; 86[h]	0.7	652/623	0.57	74[i]
8b	Me_2Sn1	−461.5	*k*	*l*	*l*	1.18	114[i]
	Me_2Sn2	−156.8	102[h]	*l*	*l*	0.70	79[i]
	Me_2Sn3	−137.6	340[h]; 103[h]	*l*	*l*	0.59	77[i]

[a] Chemical shift data in ppm and coupling constants (in Hz). [b] ^{119}Sn resonances were referenced to the absolute frequency of Me_4Sn (37.290 665 MHz[9]); see Experimental Section. [c] Combined $^{3}J(^{119}Sn1-N18-O19-^{119/117}Sn3)$ and $^{2}J(^{119}Sn1-O30-^{119/117}Sn3)$ coupling pathways, double $^{2}J(^{119}Sn2-O30-^{119/117}Sn3)$ and $^{2}J(^{119}Sn2-O40-^{119/117}Sn3)$ coupling pathways, and double $^{2}J(^{119}Sn1-O30-^{119/117}Sn2)$ and $^{2}J(^{119}Sn1-O10-^{119/117}Sn2)$ coupling pathways. [d] ^{13}C chemical shifts referenced to the solvent ($CDCl_3$) ^{13}C resonance and converted to the standard Me_4Si scale by adding 77.0 (128.0 ppm for C_6D_6). [e] Resolved $^{1}J(^{13}C-^{119}Sn)$ and $^{1}J(^{13}C-^{117}Sn)$ coupling satellites. [f] ^{1}H chemical shifts referenced to the residual solvent ($CDCl_3$) ^{1}H resonance and converted to the standard Me_4Si scale by adding 7.24 ppm (7.15 ppm for C_6D_5H). [g] Pure $^{2}J(^{1}H-^{119}Sn)$ coupling constants determined from cross sections along the F2 axis (^{1}H nuclei) of 2D $^{1}H-^{119}Sn$ HMQC spectra at the ^{119}Sn resonance frequency along the F1 axis of the corresponding tin atom. [h] Averaged values from unresolved $^{n}J(^{119}Sn-^{119}Sn)$ and $^{n}J(^{119}Sn-^{117}Sn)$ coupling satellites in ^{119}Sn spectra. [i] Averaged values from unresolved $^{2}J(^{1}H-^{119}Sn)$ and $^{2}J(^{1}H-^{117}Sn)$ coupling satellites in standard ^{1}H spectra. [j] Nonresolved coupling. [k] Not observed. [l] ^{13}C spectrum not interpretable because **8b** only observed in mixture.

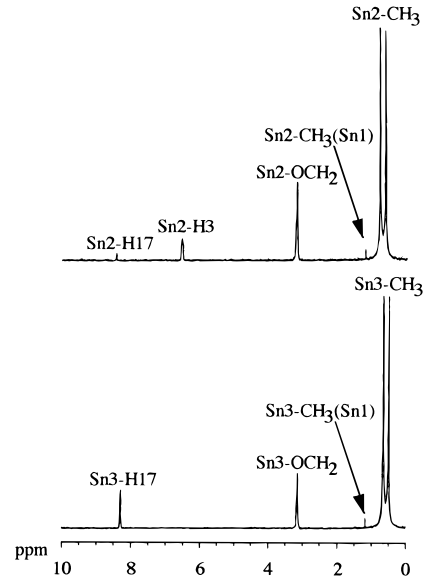

Figure 6. Data from the 2D gradient-assisted[2] $^{1}H-^{119}Sn$ HMQC spectrum[1,3a,4] of the filtrate of the crude reaction mixture obtained from the reaction of **3a** with ethylene glycol and containing **2a**, **2b**, and **8b**. The figure shows the cross sections, along the F2 (^{1}H chemical shift axis) at the ^{119}Sn resonance frequencies of the two five-coordinate tin atoms Sn2 (top) and Sn3 (bottom) of **8b**. Each signal corresponds to a ^{1}H resonance from the proton indicated, which is coupled to the ^{119}Sn nucleus of the tin atom indicated, all other ^{1}H resonances being suppressed by the gradient pulse and phase cycling schemes.[1b,4]

minor species m_2 (*ca.* −125 and −219 ppm) and m_3 (*ca.* −283 ppm), are again observed, to variable extents, in the ^{119}Sn spectra of pure **4** and **5a**−**e**, as in any solution of such clusters.[1]

The ^{119}Sn chemical shifts of the tin atoms Sn2 and Sn3 of **5a**−**e** are markedly high-frequency-shifted with respect to those of **3a**−**d** (see Table 2 and ref 1b). This deshielding effect in **5a**−**e** as compared to **3a**−**d** is attributed to the inductive electronic-withdrawing effect of the phenoxy group of **5a**−**e**, as compared to the inductive electronic releasing effect of the alkoxy group of **3a**−**d**. In addition, the ^{119}Sn chemical shifts of the substituted phenoxy derivatives **5** display a deshielding effect in the order **5e** < **5a** < **5b** < **5c** < **5d** (Table 2). This deshielding effect parallels the pK_a series of the associated phenols, confirming that the deshielding trend is associated with the increasing electron-withdrawing effect of the substituted phenyl group linked to O40.

The ^{119}Sn chemical shifts of **4** (Sn1, −452.2; Sn2, −125.6; Sn3, −112.6 ppm) are remarkably close to those of **2b** (Sn1, −451.4; Sn2, −122.9; Sn3, −109.1 ppm),[1b] suggesting these values to be characteristic of the bonding mode of the aromatic oximate ligand to the Sn2−O40−Sn3 bridge through the oximic oxygen.

NMR Characterization of 6a and 6b. The solution ^{1}H and ^{13}C NMR data found for **6a** (see Experimental Section) are in good agreement with the data reported by Lockhart et al.[5a] The ^{119}Sn NMR spectrum of **6a** in solution reveals two equally intense ^{119}Sn resonances at −173.8 and −190.2 ppm, with the latter being broad, an observation also in good agreement with literature data (−174.4 and −190.0 ppm).[5j] They are assigned to the tin atoms of the structure shown in Figure 3, known to be the most common structure, both in the solid and the solution states.[5b−j,10] The ^{119}Sn chemical shift values indeed favor five-coordination at both tin atoms rather than six-coordination.[5b−j,9c] The assignment of low- and high-frequency ^{119}Sn resonances to the exo (Sn2) and

endo (Sn1) tin atoms of the structure, conflicting in the literature,[5e,j,10a] and given in the Experimental Section, has been achieved by a 2D gradient-assisted $^{1}H-^{119}Sn$ HMQC experiment.[10c] A similar assignment is proposed for **6b**, the ^{119}Sn chemical shifts (−179.4 and −190.1 ppm) being very similar to those of **6a**, and the low-frequency ^{119}Sn resonance being again broader.

The high-frequency ^{119}Sn signal around −175 ppm exhibits unresolved $^{2}J(^{119}Sn-O-^{119/117}Sn)$ coupling satellites of 110 Hz for **6a** (103 Hz[5j]) and of 101 Hz for **6b**, which are invisible for the broad low-frequency ^{119}Sn resonance at −190 ppm. The latter is indicative of some fluxionality, different from the one previously invoked[5e,10b] since it involves only the endo tin atom. Its nature is discussed elsewhere.[10c] The ^{1}H and ^{13}C resonances of **6b** have been assigned by 2D $^{1}H-^{13}C$ HMBC and HMQC experiments.

NMR Characterization of 7 and 8a. Compound **7**, $Me_2Sn(acac)_2$, has been characterized readily from ^{1}H, ^{13}C, and ^{119}Sn NMR data in $CDCl_3$, by comparison with literature data,[7a−d] and by elemental analysis. The ^{119}Sn chemical shift of −365.9 ppm (−365 ppm[7c]) as well as the $^{1}J(^{13}C-^{119}Sn)$ coupling constant of 978 Hz (977 Hz[7c]) and the $^{2}J(^{1}H-^{119}Sn)$ coupling constant of 96 Hz (99 Hz[7d]) are in agreement with the previously described[7a,b] six-coordinate, distorted octahedral structure with the two methyl groups in a trans configuration, the bond angle Me−Sn−Me being, nevertheless, only 162.5° in solution.[7d] ^{1}H and ^{13}C NMR data are found in the Experimental Section.

Compound **8a**, 2,2-dimethyl-1,3-dioxa-2-stannacyclopentane, was characterized by NMR, mass spectrometry, and elemental analysis, in part by comparison with literature data.[8] Its extremely low solubility allowed only the recording of ^{1}H and ^{119}Sn NMR spectra in a very diluted CD_3OD solution. An unresolved $^{2}J(^{1}H-^{119/117}Sn)$ coupling constant of *ca.* 72 Hz can be recognized in its ^{1}H spectrum. Only a very broad and noisy ^{119}Sn resonance is observed for **8a** in its ^{119}Sn spectrum around −130 ppm, probably as a consequence of aggregation equilibria well established for the better soluble di-*n*-butyltin analog.[8a,c] Further indirect evidence for this interpretation is the observation of a single ^{119}Sn resonance at −234 ppm in the solid state, at significantly lower frequency as compared to the solution state. This indicates a relatively high aggregation degree for **8a**, as already proposed for the di-*n*-butyltin analog[8a] ($\delta^{119}Sn = -231$).[8c]

Experimental Section

Syntheses. Compound 4. In a round-bottomed flask equipped with a condenser and a Dean−Stark apparatus, 2.00 g of **3a** (2.6 mmol) and 0.38 g of benzaldoxime (20% molar excess) are refluxed for 5 h in benzene under distillation of the azeotrope benzene−methanol. The condenser is equipped with a $CaCl_2$ tube, in order to avoid moisture in the reaction mixture. The reaction mixture is magnetically stirred for another 24 h and subsequently evaporated. The white powder is recrystallized from a mixture of hexane/benzene 1:1 (v/v).

Compounds 5a−e. To a solution of 250 mg of **3a** (0.33 mmol) in *ca.* 50 mL of benzene stirred magnetically were added dropwise 35 mg of *p*-cresol (for **5a**), 57 mg of *p*-bromophenol (for **5b**), 45 mg of *m*-chlorophenol (for **5c**), 47 mg of *m*-nitrophenol (for **5d**), and 40 mg of 3,5-dimethylphenol (for **5e**) dissolved in 20 mL of benzene. The mixture was stirred for 24 h at room temperature and evaporated under vacuum. Crude, solid **5a** and **5b** were recrystallized from benzene/hexane 3:1 (v/v), **5c** and **5d** from dichloromethane/hexane 4:1 (v/v), and **5e** from dichloromethane/hexane 1:2 (v/v) or benzene/hexane 1:5 (v/v).

Compounds 8a and 8b. A solution of 1 g (1.3 mmol) of **3a** in 30 mL of benzene is added dropwise to 262 mg (4.2 mmol) of ethylene glycol. After stirring magnetically the mixture for 18 h, the precipitate obtained is filtered off, washed with benzene, dichloromethane, diethyl ether, and then dried to yield 530 mg of **8a**. The filtrate is evaporated to a mixture that could not be purified further, either by crystallization (oil) or by chromatography (decomposition). NMR analysis, as presented in Results and Discussion, reveals it to consist of a mixture of **2a**, **2b**, and the new compound **8b**, formally identified by $^{1}H-^{119}Sn$ HMQC spectroscopy.

Compound 6a. From 3a. To a solution of 500 mg (0.65 mmol) of **3a** in 50 mL benzene is added dropwise 39 mg of acetic acid (0.65 mmol) in 20 mL of benzene. After 24 h of magnetic stirring at room temperature, a white precipitate is formed. The precipitate is filtered off and recrystallized in dichloromethane/hexane 3:1 (v/v) to pure **6a**.

Compound 6a. From Me_2SnO. To a solution of 364 mg (6.1 mmol) of acetic acid in 140 mL of toluene/ethanol 3:1 (v/v) is added 1 g of dimethyltin oxide (6.1 mmol). After 20 min of refluxing of the heterogeneous reaction mixture, the mixture became homogeneous and is refluxed for another 6 h. The ternary followed by the binary azeotrope is distilled off with a Dean−Stark apparatus until 50% volume reduction. The remaining solution is evaporated at the Rotavapor, and the residue obtained is crystallized twice from dichloromethane/hexane 3:1 (v/v) to pure **6a**.

Compound 6b. To a solution of 500 mg (0.65 mmol) of **3a** in 50 mL of dichloromethane is added dropwise 89 mg of *p*-toluic acid (0.65 mmol) in 20 mL of dichloromethane. After 24 h of magnetic stirring at room temperature, a white precipitate is formed. The precipitate is filtered off and recrystallized in dichloromethane/hexane 3:1 (v/v) to pure **6b**.

Compound 7. To a solution of 1.528 g (2 mmol) of **3a** in 40 mL of benzene is added dropwise a solution of 1.202 g of acetylacetone (12 mmol) in 10 mL of benzene. After 20 h of magnetic stirring at room temperature, the solvent is partially evaporated under vacuum and the residue recrystallized from benzene to pure **7**.

Characterization. Mössbauer parameters (in mm/s): IS, isomer shift, ref $Ca^{119}SnO_3$; QS, quadrupole splitting; Γ, line widths. NMR data in $CDCl_3$ (except C_6D_6 for **8b**), chemical shifts in ppm; coupling constants in hertz. For references, see footnotes, Table 2. Multiplicity patterns in ^{1}H spectra: br, broad; d, doublet; dd, doublet of doublets; ddd, doublet of doublets of doublets; q, quartet; s, singlet; t, triplet; m, complex pattern; nr, nonresolved. $^{n}J(^{1}H-^{1}H)$ coupling constants are given in brackets. ^{1}H chemical shifts, $^{2}J(^{1}H-^{119}Sn)$ coupling constants, ^{13}C chemical shifts, $^{1}J(^{13}C-^{119/117}Sn)$ coupling constants for the tin methyl groups, and the ^{119}Sn chemical shifts and $^{n}J(^{119}Sn-^{119/117}Sn)$ coupling constants are given in Table 2 and not repeated here.

Compound 4. Yield 73%; mp 139−141 °C. Anal. Found: C, 40.3; H, 4.3; N, 4.6. Calcd for $C_{27}H_{35}O_6N_3Sn_3 \cdot 0.5C_6H_6$: C, 40.4; H, 4.3; N, 4.7. Mössbauer: IS 1.32, 1.11; QS 4.11, 2.89 (Γ 0.85). ^{1}H NMR: H3 6.23, d [8]; H3′ 7.08, nr m; H3″ 7.01 nr m; H4 7.01, nr m; H4′ 7.04, nr m; H4″ 7.09 nr m; H5 6.61, dd [7,7]; H5′ 6.57, dd [7,7]; H5″ 7.01 nr m; H6 6.84, d [8]; H6′ 6.82, d [8]; H2″, H6″ 7.46−7.50, nr m; H7 8.15, s; H17 8.24, s; H27 7.80, s; OH9 13.86, s. ^{13}C NMR: C1 120.6; C1′ 119.2; C1″ 129.9; C2 160.6; C2′ 162.5; C2″ 126.8; C3 117.8; C3′ 120.9; C3″ 128.8; C4 131.1; C4′ 132.7; C4″ 129.0; C5 117.5; C5′ 117.4; C5″ 128.8; C6 135.6; C6′ 132.2; C6″ 127.0; C7 150.0; C17 155.3; C27 152.9.

Compound 5a. Yield 55%; mp 107−109 °C. Anal. Found: C, 40.8; H, 4.5; N, 3.1. Calcd for $C_{27}H_{36}O_6N_2Sn_3 \cdot 0.5C_6H_6$: C, 41.2; H, 4.4; N, 3.2. Mössbauer: IS 1.40, 1.20; QS 4.11, 2.90 (Γ 0.87). ^{1}H NMR: H3 6.35, d [8]; H3′ 6.84, d

[8]; H4 7.15, ddd [8,8,2]; H4′ 7.23, ddd [8,8,2]; H5 6.75, dd [8,8]; H5′ 6.73, dd [8,8]; H6 7.13, dd [8,2]; H6′ 7.06, d [8,2]; H7 8.03, s; H17 8.17, s; Ho 6.57, d [8], 2H; Hm 7.03, d [8], 2H; CH_3 2.28, 3H, s; OH9 13.35, br s. ^{13}C NMR: C1 119.8; C1′ 118.4; C2 159.9; C2′ 161.7; C3 117.4; C3′ 120.4; C4 131.1; C4′ 132.2; C5 117.1; C5′ 117.0; C6 135.0; C6′ 131.8; C7 149.6; C17 155.0; ipso 154.0; ortho 119.7; meta 130.2; para 129.7; CH_3 20.4.

Compound 5b. Yield 68%; mp 129−131 °C. Anal. Found: C, 36.6; H, 4.0; N, 2.9. Calcd for $C_{26}H_{33}O_6N_2Sn_3Br\cdot 0.5C_6H_6$: C, 36.9; H, 3.8; N, 3.0. Mössbauer: IS 1.33, 1.14; QS 4.19, 2.98 (Γ 0.80). ^1H NMR: H3 6.31, d [8]; H3′ 6.81, d [8], H4, H4′, H6, H6′ 7.07−7.24, nr m, 4H; H5 6.73, dd [7,7]; H5′ 6.76, dd [7,7]; H7 8.01, s; H17 8.15, s; Ho 6.51, d [9], 2H; Hm 7.29, d [9], 2H, OH9 13.31, br s. ^{13}C NMR: C1 120.6; C1′ 119.9; C2 159.9; C2′ 161.7; C3 118.6; C3′ 121.8; C4 131.3; C4′ 132.5; C5 117.4; C5′ 117.3; C6 135.3; C6′ 132.0; C7 149.9; C17 155.4; ipso 156.0; ortho 117.5; meta 132.8; para 112.5.

Compound 5c. Yield 71%; mp 160−162 °C. Anal. Found: C, 36.2; H, 3.9; N, 3.2. Calcd for $C_{26}H_{33}O_6N_2Sn_3Cl$: C, 36.3; H, 3.9; N, 3.3. Mössbauer: IS 1.29, 1.17; QS 4.12, 2.91 (Γ 0.96). ^1H NMR: H3 6.38, d [8]; H3′ 6.87, d [8], H4 7.19 nr m; H4′ 7.27, dd [8,8]; H5 6.81, dd [8,8]; H5′ 6.78, dd [8,8]; H6 7.20 nr m; H6′ 7.13, br d [8]; H7 8.03, s; H17 8.17, s; Ho 6.66, s; Ho′ 6.56, d [8]; Hm′ 7.17, nr m; Hp 6.91, d [8]; OH9 13.26, br s. ^{13}C NMR: C1 120.0; C1′ 118.6; C2 159.9; C2′ 161.8; C3 117.5; C3′ 120.5; C4 131.3; C4′ 132.4; C5 117.5; C5′ 117.2; C6 135.2; C6′ 132.0; C7 149.8; C17 155.4; ipso 158.0; ortho 120.2; ortho′ 118.2; meta 135.1; meta′ 130.6; para 120.5.

Compound 5d. Yield 67%; mp 185−188 °C. Anal. Found: C, 35.8; H, 4.0; N, 4.7. Calcd for $C_{26}H_{33}O_8N_3Sn_3$: C, 35.8; H, 3.8; N, 4.8. Mössbauer: IS 1.29, 1.12; QS 3.96, 2.93 (Γ 0.81). ^1H NMR: H3 6.34, d [8]; H3′ 6.83, d [8]; H4, H6 7.15−7.18, nr m, 2H; H4′ 7.22−7.24, m; H5 6.78, dd [8,8]; H5′ 6.74, dd [8,8]; H6′ 7.10, br d [8]; H7 8.03, s; H17 8.17, s; Ho 7.43, br s; Ho′ 7.72, br d [8]; Hm′ 7.34, dd [8,8]; Hp 6.92, br d [8]; OH9 13.23, br s. ^{13}C NMR: C1 119.9; C1′ 118.5; C2 159.6; C2′ 161.7; C3 117.5; C3′ 120.5; C4 131.4; C4′ 132.6; C5 117.7; C5′ 117.4; C6 135.3; C6′ 132.0; C7 149.8; C17 155.6; ipso 149.6; ortho 114.1; ortho′ 114.8; meta 158.3; meta′ 130.3; para 126.0.

Compound 5e. Yield 91%; mp 100−103 °C. Anal. Found: C, 39.5; H, 4.6; N, 3.3. Calcd for $C_{28}H_{38}O_6N_2Sn_3$: C, 39.4; H, 4.5; N, 3.3. Mössbauer: IS 1.33; 1.08; QS 3.99, 2.73 (Γ 0.96). ^1H NMR: H3 6.11, d [8]; H3′, H4, H4′, H6, H6′ 6.79−7.09 nr m, 5H; H5, H5′ 6.59−6.62 nr m, 2H; H7 8.12, s; H17 8.17, s; Ho 6.31, s, 2H; Hp 6.53, s; CH_3 2.16, s, 6H; OH9 13.80, br s. ^{13}C NMR: C1 120.6; C1′ 119.2; C2 160.5; C2′ 162.5; C3 117.8; C3′ 120.9; C4 131.1; C4′ 132.6; C5 117.5; C5′ 117.4; C6 135.5; C6′ 132.2; C7 150.0; C17 155.2; ipso 157.0; ortho 118.6; meta 139.5; para 122.9; CH_3 21.5.

Compound 6a. Yield 77% from **3a** and 74% from $(CH_3)_2SnO$; mp 238−241 °C, respectively, 240−242 °C (lit.[5a] mp 240 °C). Anal. Found: C, 22.5; H, 4.3. Calcd for $C_{16}H_{36}O_{10}Sn_4$: C, 22.3; H, 4.2. Mössbauer: IS 1.20; QS 3.57 (Γ_1 1.01, Γ_2 0.91). ^1H NMR: CH_3C 1.92, 12H; CH_3Sn1 0.81, s [$^2J(^1H-^{119/117}Sn)$ = 91/87], 12H; CH_3Sn2 0.79, s [$^2J(^1H-^{119/117}Sn)$ = 87/83], 12H; (lit.[5a] CH_3Sn1 and CH_3Sn2 0.79 [$^2J(^1H-^{119}Sn)$ = 89.0] and 0.77 [$^2J(^1H-^{119}Sn)$ = 86.8]. ^{13}C NMR: CH_3C 22.9; CO 177.6; CH_3Sn1 and CH_3Sn2 8.7 [$^1J(^{13}C-^{119/117}Sn)$ = 802/768] and 5.9 [$^1J(^{13}C-^{119/117}Sn)$ = 752/713]; (lit.[5a] CH_3Sn1 and CH_3Sn2 5.9 [$^1J(^{13}C-^{119}Sn)$ = 748] and 8.7 [$^1J(^{13}C-^{119}Sn)$ = 800]. ^{119}Sn NMR: Sn1 −190.2 (br; $^2J(^{119}Sn-^{119/117}Sn)$ unresolved); Sn2 −173.8 [$^2J(^{119}Sn-^{119/117}Sn)$ = 110].

Compound 6b. Yield 44%; mp 208−210 °C. Anal. Found: C, 41.3; H, 4.7. Calcd for $C_{40}H_{52}O_{10}Sn_4$: C, 41.1; H, 4.5 Mössbauer: IS 1.19; QS 3.28 (Γ_1 1.02, Γ_2 0.87). ^1H NMR: *p*-CH_3 2.40, 12H; Ho 7.87, d [8], 8H; Hm 7.23, d [8], 8H; CH_3Sn1 0.99, s [$^2J(^1H-^{119}Sn)$ 92], 12H; CH_3Sn2 0.94, s [$^2J(^1H-^{119}Sn)$ 90], 12H. ^{13}C NMR: *p*-CH_3 21.7; CO 173.2; ipso 129.0; ortho 130.4; meta 129.9; para 142.8; CH_3Sn1 7.0 [$^1J(^{13}C-^{119/117}Sn)$ = 770/734]; CH_3Sn2 10.0 [$^1J(^{13}C-^{119/117}Sn)$ = 818/783]. ^{119}Sn NMR: Sn1 −190.1 (br; $^2J(^{119}Sn-^{119/117}Sn)$ unresolved); Sn2 −179.4 [$^2J(^{119}Sn-^{119/117}Sn)$ = 101].

Compound 7. Yield 56%; mp >300 °C (lit.[7b] mp >300 °C. Anal. Found: C, 41.6; H, 6.0. Calcd for $C_{12}H_{20}O_4Sn$: C, 41.5; H, 5.8. Mössbauer: IS 1.17; QS 3.94 (Γ_1 0.97, Γ_2 0.93) (lit.[7g] IS 1.20; QS 3.94 (T = 110 K)). ^1H NMR: CH_3C 1.67, s, 12H; =CH 5.02, s, 2H; CH_3Sn 0.90, s [$^2J(^1H-^{119/117}Sn)$ = 96/92], 6H (lit.[7d] [$^2J(^1H-^{119}Sn)$ = 99]). ^{13}C NMR: CH_3C 28.1; CO 190.8; =CH 100.2; CH_3Sn 7.8 [$^1J(^{13}C-^{119/117}Sn)$ = 978/936] (lit.[7c] [$^1J(^{13}C-^{119}Sn)$ = 977]). ^{119}Sn NMR: −365.9; (lit.[7c] −365.

Compound 8a. Yield 65%; mp >300 °C. Anal. Found: C, 23.3; H, 5.1. Calcd for $C_4H_{10}O_2Sn$: C, 23.0; H, 4.8. Mössbauer: IS 1.09; QS 3.01 (Γ_1 1.08, Γ_2 1.07). MS: M + 1, 211. ^1H NMR: CH_2 3.60, s, 4H; CH_3Sn 0.60, s, 6H [$^2J(^1H-^{119/117}Sn)$ = 72 unresolved]. ^{119}Sn NMR: *ca.* −130 (very br). ^{119}Sn CP MAS NMR: −234. ^{13}C CP MAS NMR: CH_2 62.0; CH_3Sn 7.2 [$^1J(^{13}C-^{119}Sn)$ = 808] 5.5 [$^1J(^{13}C-^{119}Sn)$ = 845].

Compound 8b. NMR characterization in reaction mixture containing also **2a** and **2b** by $^1H-^{119}Sn$ HMQC NMR: $^{119}Sn1$ −461.5, correlated with ^1H, H7 8.20, s; H17 8.30, s; OH(9) 14.03, s; CH_3 1.18, s. $^{119}Sn2$ −156.8, correlated with ^1H, H17 8.30, s; H3 6.44, d [7]; CH_3 0.70, s; CH_3-Sn1 1.18, s; OCH_2 3.14, s. $^{119}Sn3$ −137.6, correlated with ^1H, H17 8.30, s; CH_3 0.59, s; CH_3-Sn1 1.18, s; OCH_2 3.14, s.

Crystallography. Intensity data for the colorless crystals of **4**, **5a**, and **5b**, each isolated as a hemi-benzene solvate, were measured at room temperature (20 °C) on a Rigaku AFC6R diffractometer fitted with graphite-monochromatized Mo Kα radiation, λ = 0.710 73 Å. The ω:2θ scan technique was employed to measure data up to a maximum Bragg angle of 27.5°; the data sets were corrected for Lorentz and polarization effects[11] and an empirical absorption correction was applied in each case.[12] In the case of **4**, significant decomposition (*ca.* 20%) of the crystal occurred during the data collection, and hence, a correction was applied to the data set by assuming a linear decay. Relevant crystal data are given in Table 3. The structures were solved by direct-methods employing DIRDIF92,[13a] SIR88,[13b] and SHELXS86[13c] for **4**, **5a**, and **5b**, respectively, and each refined by a full-matrix least-squares procedure based on F.[11] Non-H atoms were refined with anisotropic displacement parameters, and H atoms were included in the models in their calculated positions (C−H 0.97 Å); the OH hydrogen atom was located in the refinement of both **4** and **5b** but not for **5a**. The refinements were continued until convergence by employing σ weights (i.e., $w = 1/\sigma^2(F)$) and the analysis of variance showed no special features, indicating that an appropriate weighting scheme had been applied in each case. Final refinement details are collected in Table 3. The numbering schemes employed are shown in Figures 5, 6 and S(1), which were drawn with ORTEP[14] at 30% probability ellipsoids. The teXsan[11] package, installed on an Iris Indigo workstation, was employed for all calculations.

(9) (a) Mason, J. *Multinuclear NMR*; Plenum Press: New York, 1987; pp 625−629. (b) Davies, A. G.; Harrison, P. G.; Kennedy, J. D.; Puddephatt, R. J.; Mitchell, T. N.; McFarlane, W. *J. Chem. Soc. A* **1969**, 1136. (c) Wrackmeyer, B. *Annu. Rep. NMR Spectrosc.* **1985**, *16*, 73.

(10) (a) Vatsa, C.; Jain, V. K.; Kesavadas, T.; Tiekink, E. R. T. *J. Organomet. Chem.* **1991**, *408*, 157. (b) Gross, D. C. *Inorg. Chem.* **1989**, *28*, 2355. (c) Ribot, F.; Sanchez, C.; Meddour, A.; Gielen, M.; Tiekink, E. R. T.; Biesemans, M.; Willem, R. *J. Organomet. Chem.*, submitted for publication.

(11) teXsan: Structure Analysis Software. Molecular Structure Corp., The Woodlands, TX.

(12) Walker, N.; Stuart, D. *Acta Crystallogr., Sect. A* **1983**, *39*, 158.

(13) (a) Beurskens, P. T.; Admiraal, G.; Beurskens, G.; Bosman, W. P.; Garcia-Granda, S.; Smits, J. M. M.; Smykalla, C. The DIRDIF program system, Technical Report of the Crystallography Laboratory, University of Nijmegen, The Netherlands, 1992. (b) Burla, M. C.; Camalli, M.; Cascarano, G.; Giacovazzo, C.; Polidori, G.; Spagna, R.; Viterbo, D. *J. Appl. Crystallogr.* **1989**, *22*, 389. (c) Sheldrick, G. M. SHELXS86, Program for the Automatic Solution of Crystal Structure, University of Göttingen, Germany, 1986.

(14) Johnson, C. K. ORTEP. Report ORNL-5138, Oak Ridge National Laboratory, TN, 1976.

Table 3. Crystallographic Data and Refinement Details for 4, 5a, and 5b

	4	5a	5b
formula	$C_{30}H_{38}N_3O_6Sn_3$	$C_{30}H_{39}N_2O_6Sn_3$	$C_{29}H_{36}BrN_2O_6Sn_3$
fw	892.7	879.7	944.6
cryst size, mm	0.08 × 0.32 × 0.32	0.13 × 0.29 × 0.29	0.16 × 0.16 × 0.24
cryst syst	triclinic	triclinic	triclinic
space group	$P\bar{1}$	$P\bar{1}$	$P\bar{1}$
a, Å	12.334(5)	11.744(5)	11.765(9)
b, Å	14.624(7)	15.768(5)	15.76(1)
c, Å	10.101(3)	10.200(4)	10.205(8)
α, deg	103.00(3)	105.10(3)	105.09(7)
β, deg	102.90(2)	112.88(3)	113.43(6)
γ, deg	86.63(4)	87.30(3)	87.26(7)
V, Å^3	1730(1)	1677(1)	1673(2)
Z	2	2	2
D_{calcd}, g cm^{-3}	1.713	1.742	1.875
$F(000)$	874	862	914
μ, cm^{-1}	21.90	22.58	34.60
transmission factors	0.898−1	0.939−1	0.909−1
no. of data collcd	8339	8117	8098
no. of unique data	7972	7742	7724
no. of unique data with $I \geq 3.0\sigma(I)$	4821	5471	4611
R	0.039	0.037	0.038
R_w	0.039	0.044	0.034
residual electron density	0.67	0.84	0.66

NMR Experiments. The samples were prepared by dissolving *ca.* 40 mg of product in 0.5 mL of $CDCl_3$. All spectra were recorded at 303 K on a Bruker AMX500 spectrometer equipped with a digital lock and operating at 500.13, 125.77, and 186.50 MHz for ^{1}H, ^{13}C, and ^{119}Sn nuclei, respectively. Chemical shifts were referenced to the residual solvent peak ($CDCl_3$) and converted to the standard TMS scale by adding 7.23 and 77.0 ppm for ^{1}H and ^{13}C nuclei, respectively. The ^{119}Sn reference frequency was calculated from the absolute frequency of Me_4Sn, which is 37.290 665 MHz[9] at the B_0 field corresponding to 100.000 000 MHz for the ^{1}H nuclei in TMS.

Broad-band ^{1}H-decoupled ^{13}C and ^{119}Sn spectra as well as ^{13}C DEPT spectra were recorded using the Bruker pulse sequences with standard delays. All heteronuclear correlation spectroscopy consisted of gradient-enhanced[2] versions of the standard HMQC[3a] and HMBC[3b,c] pulse sequences, all processed in the magnitude mode. In particular, the gradient-enhanced[2] ^{1}H−^{119}Sn HMQC[4] and the ^{1}H−^{13}C HMBC[3b,c] experiments were implemented in exactly the same way as presented recently.[1b]

The ^{13}C and ^{119}Sn solid state NMR spectra were obtained as described previously.[15]

Routine NMR ^{1}H, ^{13}C, and ^{117}Sn NMR spectra were recorded on a Bruker AC250 instrument tuned at 250.13, 67.93, and 89.15 MHz, respectively. On this instrument, ^{117}Sn spectra were recorded instead of the more common ^{119}Sn ones to overcome a local radio interference problem.[16] No misinterpretations are to be expected when ^{117}Sn and ^{119}Sn chemical shift data are compared, since ^{117}Sn/^{119}Sn isotopic effects on tin chemical shifts are known to be negligible.[15,17] Accordingly, for reasons of presentation convenience, all tin NMR data are presented as ^{119}Sn chemical shifts.

Mössbauer Data. Mössbauer data were acquired and processed as previously described.[1a]

Acknowledgment. The financial support of the Belgian Flemish Science Foundation (FKFO, Grant 2.0094.94) and of the Belgian "Nationale Loterij" (Grant 9.0006.93) is gratefully acknowledged (R.W., M.B.). The authors are indebted to the European Union Program "Human Capital & Mobility" (R.W., C.S.) for financial support (Contract ERBCHRX-CT-94-0610). Research grants from the Australian Research Council (E.R.T.T.) are gratefully acknowledged. We thank Mrs. I. Verbruggen for recording routine NMR spectra and Dr. B. Mahieu, Université Catholique de Louvain, Louvain-la-Neuve (B), for recording the Mössbauer data. Postdoctoral grants of the Flemish "Fonds voor Wetenschappelijk Onderzoek Vlaanderen" (A.M.) and of the Mexican "Consejo Nacional de Ciencia y Tecnologia" (C.C.C) are gratefully acknowledged.

Supporting Information Available: Further details of the structure determination including atomic coordinates, bond distances and angles, and thermal parameters for **4**, **5a**, and **5b** (19 pages). Ordering information is given on any current masthead page.

OM970378E

(15) (a) Biesemans, M.; Willem, R.; Damoun, S.; Geerlings, P.; Lahcini, M.; Jaumier, P.; Jousseaume, B. *Organometallics* **1996**, *15*, 2237. (b) Dumartin, G.; Kharboutli, J.; Delmond, B.; Pereyre, M.; Biesemans, M.; Gielen, M.; Willem, R. *Organometallics* **1996**, *15*, 19.

(16) (a) Koch, B. R.; Fazakerley, G. V.; Dijkstra, E. *Inorg. Chim. Acta* **1980**, *45*, L51. (b) Harrison, P. G. In *Chemistry of Tin*; Harrison, P. G., Ed.; Blackie & Son Ltd.: Glasgow, 1989; Chapter 3, p 113.

(17) McFarlane, H. C. E.; McFarlane, W.; Turner, C. J. *Mol. Phys.* **1979**, *37*, 1639.